PERGAMON

Quaternary Science Reviews 23 (2004) 161–174

QSR

ESR dating of North Anatolian (Turkey) and Nojima (Japan) faults

Ü. Ulusoy*

Department of Physics Engineering, Hacettepe University, Beytepe, 06532 Ankara, Turkey

Received 30 April 2002; accepted 16 June 2003

Abstract

Electron spin resonance (ESR) ages were obtained on Al, E′ and OH centres in quartz extracted from fault gouge from the North Anatolian Fault (NAF) in Turkey and the Nojima Fault (NF) in Japan. The data were used to test two contradictory criteria which have been used for the recognition of complete signal resetting during the fault movement: the grain-size plateau and the isochron models. The grain-size plateau method predicts decreasing ages with decreasing gain sizes because the fine grains are more intensely stressed during the faulting process. For those grains that were completely reset, a plateau of constant age is obtained and ESR ages derived from centres with different stress sensitivity converge. The isochron method is based on the fact that newly formed fracture surfaces are exposed to external alpha and beta radiation; thus, smaller grains ought to accumulate larger dose values. The plot of grain size versus external dose rate yields an isochron which gives the age of the fracturing process. It was found that most samples yielded smaller doses with decreasing grain sizes, thus, confirming the underlying principles of the grain size plateau method. However, only one sample yielded an extended plateau over a wider particle size range and converging ages for the different centres. The E′ centre of the sample from the NF yielded the only result that indicated that the isochron method might work. The results derived from the E′ centre of the other samples may have been interferred with by the so-called counterfeit E′ signal, which may render those results unreliable.

The ESR ages obtained on the NAF, Burdigalian to Pliocene, agree with those derived from geological estimates. Sample B, which gave the extended plateaux and an age estimate of 2.54 ± 0.58 Ma, indicates the time when faulting began. The youngest age of 0.59 ± 0.1 Ma may indicate the last major faulting episode of the NAF. The minimum age of 1.56 ± 0.22 Ma obtained on the sample from the NF coincides with the commencement of the uplift of Awaji Island at about 1.2 Ma ago, which was caused by movements of the NF as well as a range of other fault systems in the area.
© 2003 Elsevier Ltd. All rights reserved.

1. Introduction

Determining the age of a fault movement is important for the risk assessment of future fault movements. Trenches across a fault region are excavated to establish the chronology of the relative displacement of the rocks. In addition to historical records, fault movements have been dated by various radiometric methods such as fission track using epidote, a secondary mineral (Bar et al., 1974), K–Ar using illites, in intrafault material (Kralik et al., 1992), uranium series using the uranium minerals carnotite and tyuyamunite (Eyal et al., 1992) as well as electron spin resonance (ESR) using gypsum (Ikeda and Ikeya, 1992). However, the materials used in these methods are less common in fault gouge and attempts to determine the absolute ages of fault movements using them have not generally been successful (Ikeya, 1993).

Quartz, one of the most common minerals in nature, has been used for ESR dating by a number of groups: Shimokawa et al. (1984) for volcanic rock; Toyoda and Ikeya (1991) for granite; Imai et al. (1985) for volcanic ash; Yokoyama et al. (1985) and Falgueres et al. (1991) for sediments; Ulusoy et al. (1996) for volcanic sediments and Ulusoy (2000) for metamorphic rocks. In this paper, quartz is used for ESR dating of fault movements. The ESR dating method assumes that the paramagnetic centres in intrafault materials are reset by shear-stress (or frictional heating caused by shearing) at the time of faulting. It is based on the detection of paramagnetic defects created by natural ionizing radiation and accumulated in minerals after faulting. The total accumulated dose for natural ionizing radiation, D_E, is obtained by additive dose method, i.e., extrapolation of signal dose–response curve to the zero

*Tel.: +90-312-297-6179; fax: +90-312-299-2037.
E-mail address: ulusoy@hacettepe.edu.tr (Ü. Ulusoy).

0277-3791/$ - see front matter © 2003 Elsevier Ltd. All rights reserved.
doi:10.1016/S0277-3791(03)00214-2

ordinate. It is converted to an ESR age, by using the equation $T = D_E/D$ where D is the dose rate calculated from concentrations of radioactive elements (^{238}U, ^{232}Th and ^{40}K). The contribution of the cosmic dose rate was calculated after Ikeya (1988).

1.1. Criteria on ESR dating of fault movements

Ikeya et al. (1982) was the first who showed that ESR dating may be used for age determinations of fault movements, assuming that the frictional stress during faulting zeroed the ESR signals of quartz. Since then many efforts have been devoted to further establish this method. Miki and Ikeya (1982) showed experimentally that crushing of quartz grains may cause a reduction in the signal intensity. Fukuchi (1988) discussed the most serious problem in the ESR dating of fault movements. Are ESR signals that had accumulated before faulting completely zeroed at the time of fault movement? Fukuchi (1989a, b) proposed "*the multiple centre method*" for fault dating, which assumes that the frictional heating caused by shearing is the main zeroing mechanism and complete zeroing is demonstrated when the equivalent doses for several ESR signals with different stabilities agree within error. Additionally, two other criteria were proposed for the recognition of complete resetting: the "grain size plateau" and "fault gouge isochron" methods.

1.1.1. Grain size plateau

This method, which was suggested by Schwarcz et al. (1987) and Buhay et al. (1988), is based on the assumption that the finer grains should have been more effectively zeroed than coarser grains. Complete zeroing can be recognized when the same ages are obtained for several grain size fractions. When a sample is exposed to sufficiently intense stress, complete resetting should lead to the establishment of a plateau of equal D_E or ESR age values for grains smaller than a particular size (Fig. 1a). Where no plateau is obtained, it can sometimes be observed that the smallest grain sizes yield convergent D_E values for centres with different stress sensitivities.

The highest probability for complete zeroing is close to a main sliding surface such as the boundary between gouge and unbroken rock. Samples of less intensely disturbed material may have only been partly reset. While samples collected at the present-day erosional surface may display a plateau, there is no guarantee that the age derived from this plateau corresponds to the latest fault movement. It may be necessary to obtain drill cores to some moderate depth in the fault zone to obtain samples that were recently reset (Buhay et al., 1988). Lee and Schwarcz (1994) reported successful results of ESR dating, with E_1', Al and oxygen hole centres in quartz extracted from fault gouge of San Gabriel fault zone, California. The ages of these centres were consistent with geologic evidence of intersecting fault traces.

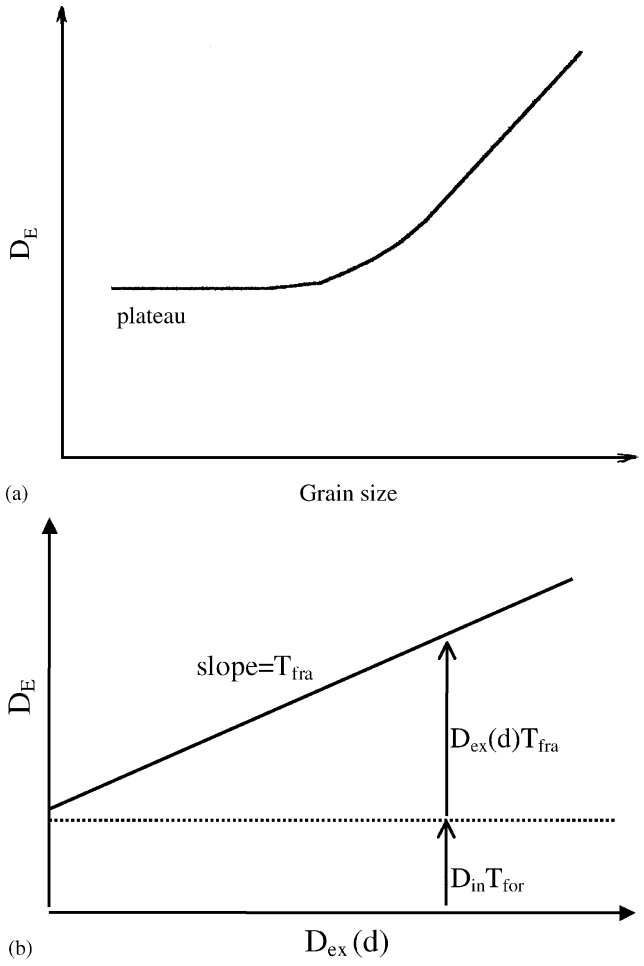

Fig. 1. (a) D_E plateau development due to grain size plateau model as grain size decreases. A wider plateau indicates complete resetting of the centre (from Buhay et al., 1988). (b) D_E of quartz grains with a diameter (d) in fault gouge as a function of corrected external annual dose ($D_{ex}(d)$) considering the range of both α- and β-rays. D_E increases by increasing $D_{ex}(d)$ (=decreasing grain size). The slope gives an age of the surface fracture (T_{fra}) and intersecting with the abscissa the dose of bulk sample since formation (from Ikeya et al., 1995).

1.1.2. Fault gouge isochron method

A coherent fault gouge isochron was proposed by Ikeya et al. (1995). In this method, fracture age is based on different dose rates for different grain sizes due to the dose attenuation factors. Fracture surfaces of grains formed in an earthquake are freshly exposed to external α- and β-rays. Consequently, D_E values increase with decreasing grain sizes. The D_E values are plotted against the external dose rates and the slope gives an isochron age for the fracturing event (Fig. 1b). The D_E is expressed by $D_E = D_{in}T_{for} + D_{ex}(d)T_{fra}$, where T_{for} is the age since the formation of quartz and T_{fra} is the fracture age. The slope gives T_{fra} and the intersection

with the abscissa yields the dose, $D_{in}T_{for}$, since formation. It is assumed that different grain sizes have been formed at the time of rock fractures during a single faulting event. In support of their theory, Ikeya et al. (1995) gave only one successful case using E′ centres in quartz from the Rokko fault in Japan.

However, grain size plateau and isochron methods contradict each other. The plateau method suggests decreasing D_E value or ESR ages with decreasing grain size whereas the isochron method proposes increasing D_E values or ESR ages with decreasing grain size. Because of this contradiction, a detailed examination of both methods is required.

The key aim of this study is to examine and compare the two models using several samples from the North Anatolian Fault (NAF) before the Izmit Earthquake ($M_w = 7.4$ on August 17, 1999) in Turkey and the Nojima Fault (NF) after the Kobe Earthquake ($M_w = 7.2$ on January 17, 1995) in Japan.

1.2. The North Anatolian Fault

The Turkish (Anatolian) subplate is located between the Eurasian, African and Arabian plates. It is squeezed and driven by the stresses exerted on it through the northward movements of the Arabian and African plates. The five major fault systems in Anatolia (the North Anatolian, East Anatolian, Bitlis, Ecemis and Tuz Gölü Faults) are located along the boundaries with those plates and in the interior of the Anatolian plate.

The NAF zone, which extends along the boundary between the Eurasian plate to the North and Anatolian plate to the South, is a major tectonic feature with a well-defined fault trace and an established history of seismicity over 1000 km long in the central portion between longitudes 31 and 41°E (Toksöz et al., 1979). To the west of 31°E longitude, the fault appears to break into two, or possibly three branches and these branches extend to Marmara Sea (Fig. 2a). The NAF zone, one of the most active zones in the world, is a natural laboratory for researchers on faulting and earthquake studies.

The age of the NAF is not exactly known. Ketin (1968, 1969) and Barka (1981) suggested that the fault has been moving since Pliocene–Quaternary era with a total displacement of a few tens of kilometers. Geological research showed that the different segments of the NAF zone might have been formed with the different slip rates at the different times. The last data presented by geologists indicated that the age of fault formation falls between Burdigalian and Pliocene Epoch (Demirtaş, 2000).

Two groups of the sampling points belong to the Almacık Ophiolite and Abant Complexes along the

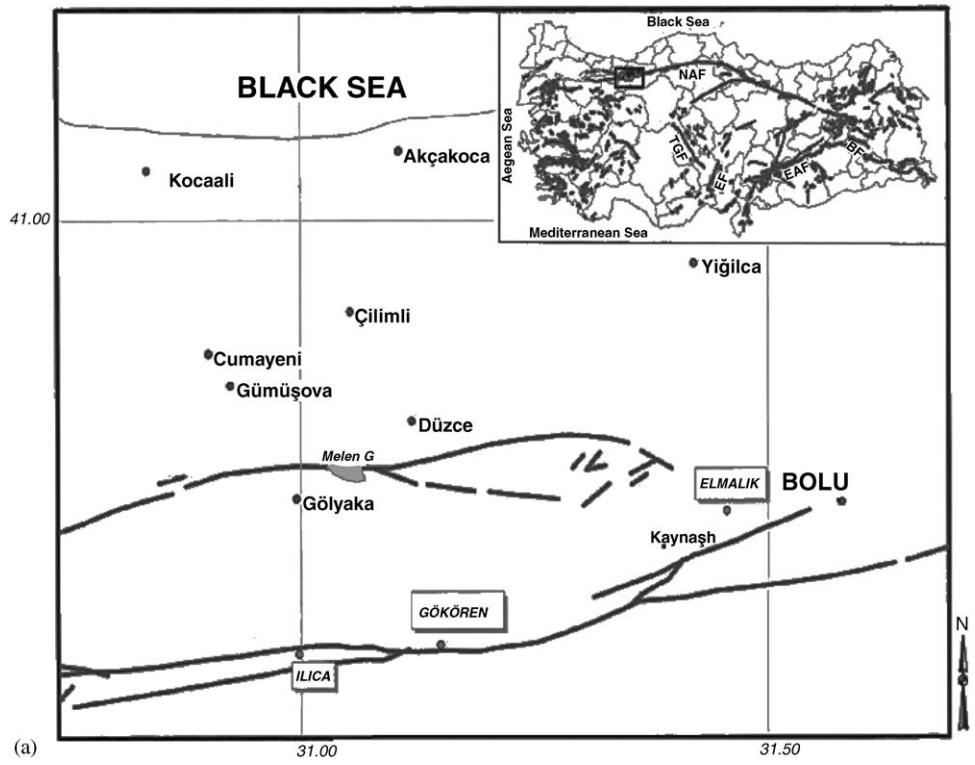

Fig. 2. (a) A part of the map of the NAF (North Anatolian Fault) showing locations of sample sites (Ilıca, Gökören of Mudurnu and Elmalık Portal of the Bolu Tunnel in Bolu). NAF: North Anatolian Fault, EAF: East Anatolian Fault, BF: Bitlis Fault, EF: Ecemiş Fault, TGF: Tuz Gölü Fault. (b) Geological map of the nothern part of Awaji Island (modified from Tadokoro et al. (2001) and Tanaka et al., 2001). N was collected from the surface outcrop of the NF (Nojima Fault) gouge at Hirabayashi.

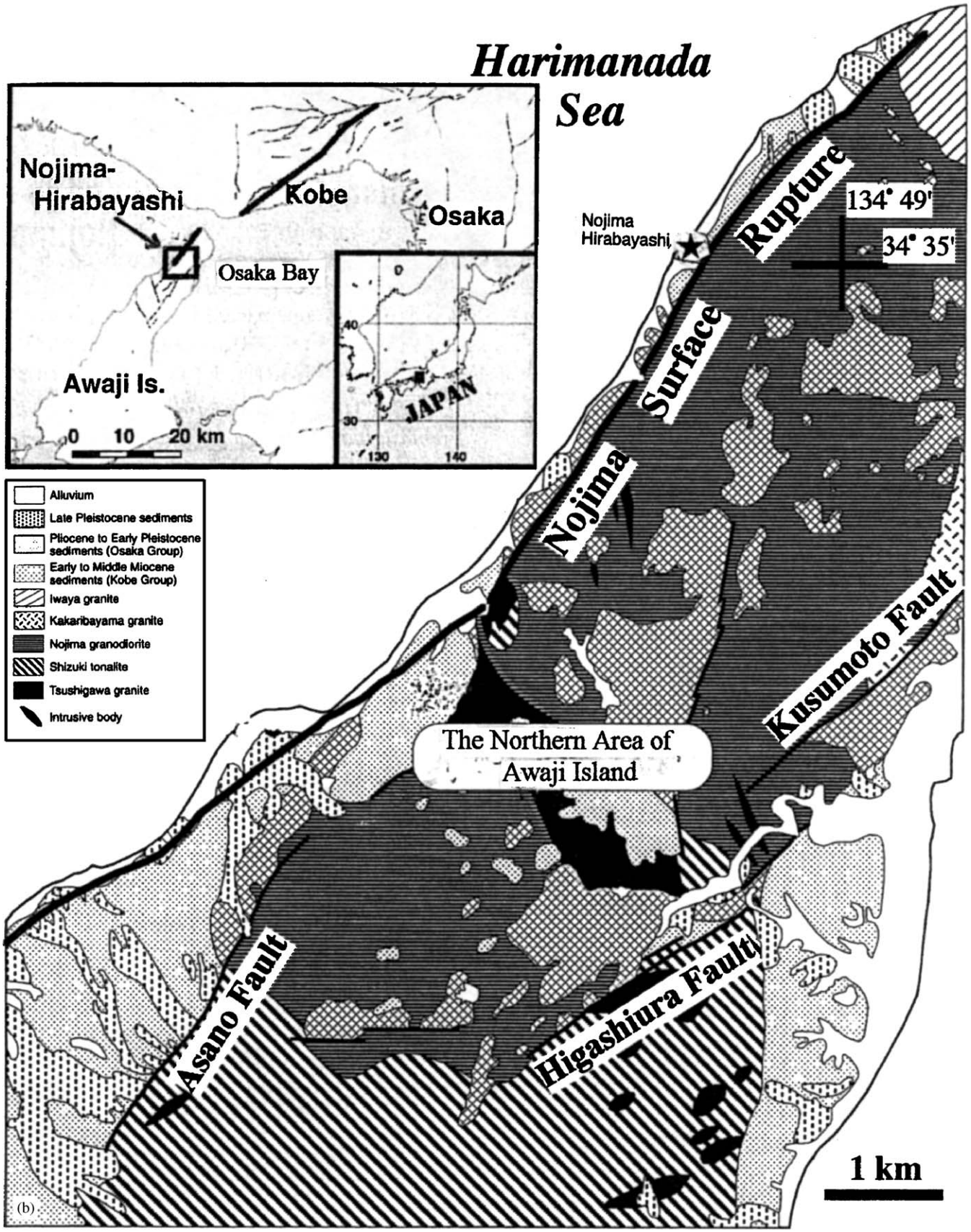

Fig. 2 (*continued*).

Mudurnu Fault. The others are in the Düzce Formation, a segment of the NAF zone, at the Düzce Fault. Mudurnu Fault at Gökören of Mudurnu in Bolu city belongs to the Abant Complex (or Arkotdağ Formation) on both sides of the NAF zone. It was activated at last the time of the Mudurnu Valley Earthquake of July 22, 1967 ($M_w = 7.1$). It has been active over the last 1.97–2.36 Ma, assuming a slip rate of 1.27 cm/a. The Mudurnu Fault at the other sampling point, at Ilıca of Mudurnu, belongs to the Almacık Ophiolite Complex (see Fig. 2a). Geological research at these segments show that the initiation age of the NAF zone ranges from the late Pliocene to Early Pleistocene Epoch (Demirtaş, 2000). The Düzce Fault was activated in the Düzce-Bolu Earthquake of November 12, 1999 ($M_w = 7.2$). As indicated by Şaroğlu et al. (1992), the fault, which is a right-lateral strike-slip fault, runs between the alluvial deposits and basement rocks in Akyazı and Düzce Plains (Aydan et al., 2000). The formation age of this fault is suggested as upper createse.

The NAF samples GK and GG were collected from the Mudurnu Fault at Ilıca of Mudurnu while the second one, GOK, was taken from the same fault at Gökören of Mudurnu in Bolu. Core samples named as B, B1, D1 and E1 were taken from various depths at the the Düzce Fault around Elmalık in Bolu, during the construction of Bolu Tunnel. The elevations of the sample areas are about 1000 m (Fig. 2a).

1.3. The Nojima Fault

Many active faults, such as Rokko active fault system, Nojima and Kusumoto Faults, and the active fault system of the Median Tectonic Line, are located in the area from Kobe, through Awaji Island and east Shikoku. They are considered to have been activated since the Middle Pleistocene.

Four active faults are known in the northern Awaji Island along the east and west coasts: the Nojima, Asano, Kusumoto and Higashiura Faults (Fig. 2b). Northern Awaji Island is considered to have been uplifted by the movement of these faults. The NF, striking north-east and dipping south-east, borders the western fringes of the mountains, and runs along the west coast of northern Awaji Island. It juxtaposes sedimentary rocks of the Miocene Kobe Group and Plio–Pleistocene Osaka Group on the west side against Cretaceous Ryoke granitic rocks on the east.

The time at which the NF was activated is a problem when estimating the average vertical slip rate from the total vertical offset. Geological research on Awaji Island showed that it started to uplift approximately 1.2 Ma ago mainly by fault movements of the Nojima, Asano, Kusumoto and Higashiura Faults (Arai and Takemura, 2001 was referred to in Murata et al., 2001).

The displacement of the NF during the Kobe Earthquake was 1–2 m right-laterally (2.1 m maximum at Hirabayashi). The north-eastern part of the NF displaced the 20,000 BP terrace surface at Hirabayashi. The average horizontal and vertical slip rates of the fault have been calculated as about 1.0 and 0.5 m/ka respectively, during the past 2000 years. The average vertical slip rate is nearly the same as that obtained for Awaji Island for the past 1.2 Ma, meaning that the activity of the north-eastern part of the NF continued from 1.2 Ma ago to the present at a nearly constant slip rate (Murata et al., 2001). The sampling area is located at Hirabayashi in the north-eastern part of the NF, which is a boundary between the granitic rocks and the Kobe-Osaka Group.

The sample N was collected from the thick layer of greyish gouge at Hirabayashi, near the centre of the NF. The elevation of the sample site is 15 m (Fig. 2b).

The properties of the samples such as origins, sampling points, depths from the surface, mineral composed and expected age in geology are shown in Table 1.

2. Experimental procedures

2.1. Sample preparation

Gouge samples have a bulk composition that contains clay, quartz, plagioclase, chlorite, lithic fragments and limestone. In order to separate quartz grains from the bulk composition, several separation techniques were used. First, all groups of the samples were immersed in water for 1 day and then washed with water in an ultrasonic cleaner to remove clay minerals. The particles with sizes smaller than 1.5 mm were selected for further separation procedures. These were washed in 10% H_2O_2 and concentrated HCl (12 M) for a few hours at room temperature to dissolve the carbonate matrix and separated from the magnetic fraction by using magnetic separation procedures. Then, they were dry sieved to fractions of <0.045, 0.045–0.075, 0.075–0.1, 0.1–0.15, 0.15–0.25, 0.25–0.5 and 0.5–1.0 mm. Finally, each grain size fraction of quartz and plagioglase grains was etched by a 40% hexafluorosilicic acid (H_2SiF_6) solution for 6 h at room temperature and then rinsed with deionized water to remove remaining plagioglase and its fine grained derivatives. HF acid was not used in this study since it affects the quartz grains. The selected sample groups named as B1, B, GG, GOK and N were nearly pure quartz except for a small amount of plagioclase (as confirmed by X-ray diffraction analysis).

For a second experiment, D1 and E1 from the Düzce Fault and GK from the Mudurnu Fault were sieved to fractions of 0.045–0.075, 0.020–0.045 and 0.045–0.075 mm, respectively after the same procedures were

Table 1
Some properties of the samples from the NAF and NF used in this study

Samples	Origin	Sampling points (depth fom surface—m)	Expected era or age	Properties of the sample
GK	Mudurnu Fault (seconder fault of the NAF) in the Almacık Ophiolite Complex	Ilıca of Mudurnu in Bolu (from surface of the side of valley)	Late Pliocene–Early Pleistocene (1.97–2.36 Ma)	Red color, containing plenty of quartz and a small amount of plagioclase
GG	Mudurnu Fault (seconder fault of the NAF) in the Almacık Ophiolite Complex	Ilıca of Mudurnu in Bolu (from surface of the side of valley)	Late Pliocene–Early Pleistocene (1.97–2.36 Ma)	Light grey color, containing plenty of quartz and rare amount of plagioclase
GOK	Mudurnu Fault in the Abant or Arkotdağ Complex	Gökören of Mudurnu in Bolu (from the surface)	Late Pliocene–Early Pleistocene (1.97–2.36 Ma)	Limestone (partly marble), white colour, containing quartz, plagioclase and calcite
B	Düzce Fault (sub-branch of the NAF) in the Düzce Formation	Elmalık Portal of the Bolu Tunnel (245)	Upper Cretaceous	Meta-sediment, faulted rock with abundant clayey fault gouge/clayey fault gouge including chloride; grey color, very hard
B1	Düzce Fault (sub-branch of the NAF) in the Düzce Formation	Elmalık Portal of the Bolu Tunnel (190)	Upper Cretaceous	Metagranodiorite, metadiorite, metagranite, granodiorite, diorite, granite
D1	Düzce Fault (sub-branch of the NAF) in the Düzce Formation	Elmalık Portal of the Bolu Tunnel (170)	Upper Cretaceous	Flyschoid series: Fault gouge clayey matrix with gravel to borders fragments of calcareaus siltstone, marl, sandstone, limestone and brecciated conglomerate. Redbrown, yellowbrown coloured. Pebble, gravel to cobbles. Sedimentary rock fragments (limestone) in sandy siltyclay to Clayey fault gouge matrix. Clay with silt, including clay 80% of total and containing plenty of quartz
E1	Düzce Fault (sub-branch of the NAF) in the Düzce Formation	Elmalık Portal of the Bolu Tunnel (90)	Upper Cretaceous	Stiff plastic clayey fault gouge and fault breccia. Dark brown coloured. Soft to stiff and plastic clayey fault gouge and fault breccia consisting of 80% clay minerals. Clay minerals are principally smectites. Clayey fault gouge is MH and OH group of soil types according to USCS and shows a rather high swelling pressure. Milonitic fault breccia containing quartz and plagioclase as main component of minerals
N	Nojima Fault	Hirabayashi (from the surface outcrop of the NF gouge)	1.2 Ma	Granodiorite on the surface, lime stone, white colour, main component of quartz and plagioclase

used as described before. Then, the samples were additionally etched in 20% HF acid solution for 2 h to remove remaining plagioclase and reduce α-dose from the host matrix. Thus, the second group samples named as D1(HF), E1(HF) and GK(HF) were assumed as having received only β- and γ-radiation.

Six to eight aliquots of 200 mg from each grain size range of the sample groups were for γ-irradiated using a ^{60}Co-source with a dose rate of 0.73 Gy/s. The dose received by the aliquots was determined with a portable dosimeter placed besides the samples during irradiation.

2.2. ESR measurements

The samples were analysed on a commercial X-band ESR spectrometer (JEOL RE-2X) with a 100 kHz field modulation. The ESR spectra of Al centres and E′, OH, Ge centres were measured at 77 K and at room

temperature with microwave power 5 and 0.01 mW; scan width 30 and 15 mT; scan speed 7.5 and 3.75 mT/min; modulation amplitude 0.1 and 0.05 mT, respectively. Time constant was 0.1s.

ESR signal intensities were measured over a range of hyperfine splitting lines between g values: 2.017–1.985 for the Al centre (Fig. 3a for N), 2.011 and 2.001 for the OH and E′ centres, respectively, (Fig. 3b for B). The Ge centre was only observed in irradiated samples at room temperature except for the B sample because of bleaching by sunlight during sample preparation, while the Ti centres were not observed in these samples. Therefore, ESR signal intensities of the Al, OH and E′ centres were measured to obtain the growth of the signals in response to the added doses. The growth curves were fitted to the data and D_E and associated errors were calculated according to Ikeya (1993). Fig. 4a and b shows the dose–response curves for Al, E′ and OH centres in B for the sizes of (0.045–0.075 mm) and (0.50–1.00 mm).

2.3. Dose rate estimation

The annual doses, D, were calculated from the concentrations of ^{238}U, ^{232}Th and K in the samples as measured by γ-ray spectroscopy (Table 2). We used conversion factors assuming radioactive equilibrium in the ^{238}U and ^{232}Th series (Ogoh et al., 1993). α- and β-attenuation factors for each grain size were taken from Mejdahl (1979) and Grün (1989) and an α-efficiency of 0.07 was used Bell (1980). Water attenuation was considered while a contribution of cosmic rays was neglected. The contents of U, Th, K_2O and water, and D and their associated errors for each sample are presented in Table 2.

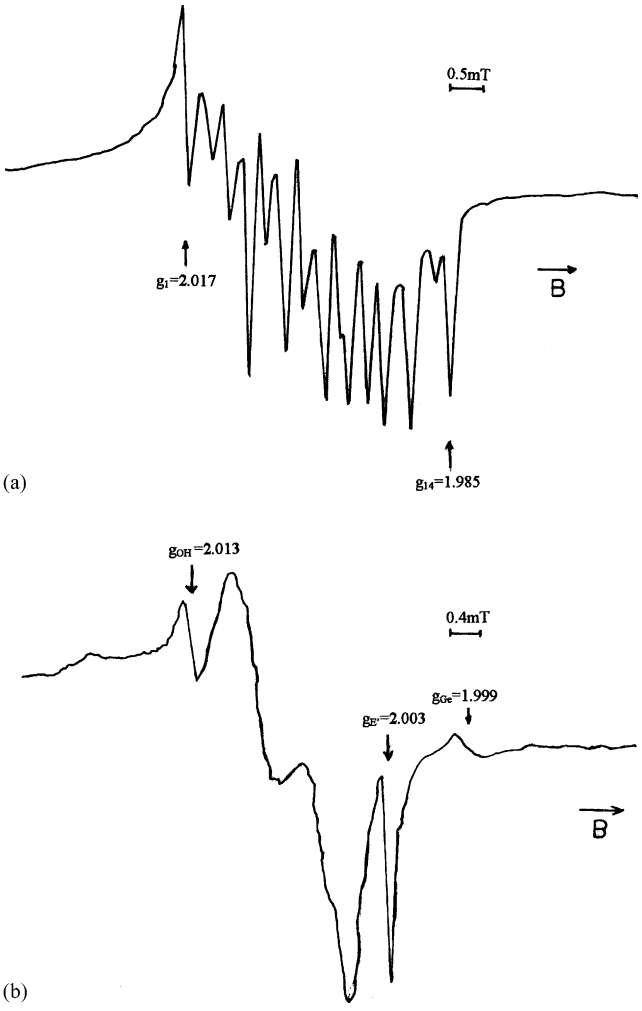

Fig. 3. ESR spectra observed in quartz extracted from the samples of fault gouge: (a) Al centres in natural N from the NF at 77 K; (b) OH and E′ centres in natural B from the Düzce Fault at the NAF at room temperatures.

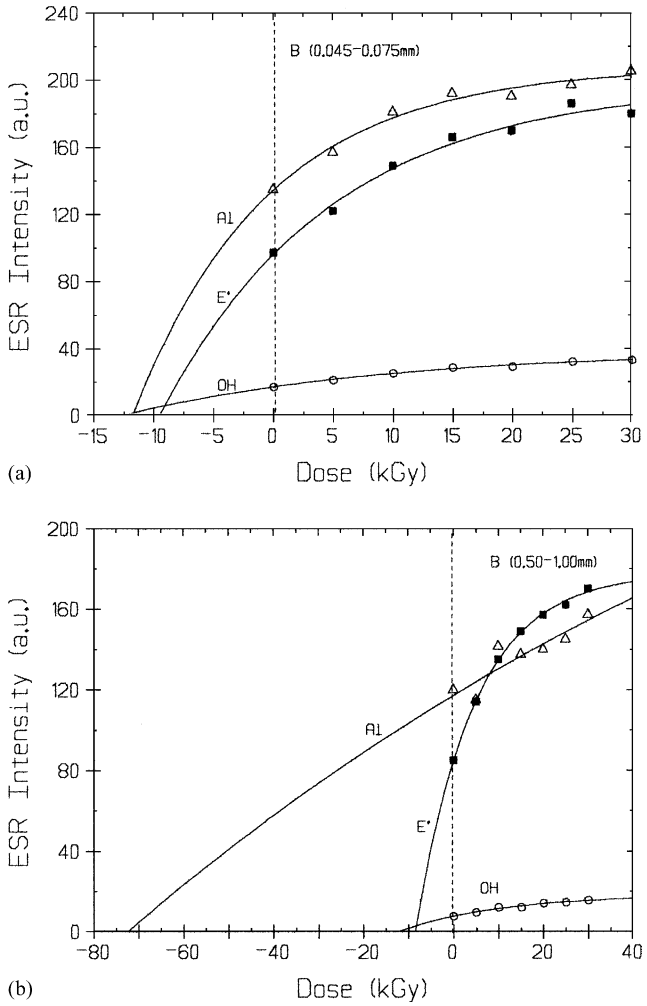

Fig. 4. Growth curves of the Al, E′ and OH centres in B from the NAF at the depth of 245 m for the sizes of (a) 0.045–0.075 mm and (b) 0.50–1.00 mm.

Table 2
ESR analytical data for fault gouge samples from the NAF and NF

Sample	Grain size (mm)	D_E (kGy)			Radioactive contents			W (%)	Dose rate (mGy/a)	T (Ma)		
		Al	E′	OH	U (ppm)	Th (ppm)	K (%)			Al	E′	OH
GG	<0.045	2.76±0.80	10.94±2.76		2.65±0.04	15.47±0.41	Not determined	8.14	2.63±0.02	1.05±0.31	4.16±1.08	
	0.045–0.075	3.64±0.61	8.70±1.56						2.10±0.02	1.73±0.31	4.14±0.78	
	0.075–0.100	4.53±1.55	12.20±4.16						1.95±0.02	2.32±0.82	6.26±2.19	
	0.100–0.150	8.37±2.28	22.45±9.55						1.88±0.02	4.45±1.26	11.94±5.20	
	0.150–0.250	10.79±8.43	0.96±6.28						1.81±0.02	5.96±4.71	0.53±3.47	
	0.250–0.500	16.33±6.67	9.69±1.69						1.75±0.02	9.33±3.93	5.54±1.03	
GK (HF)	0.045–0.075	2.56±0.45	11.07±3.50		2.31±0.04	0.54±0.13	2.47±0.05	7.67	2.48±0.03	1.03±0.19	4.46±1.48	
GOK	0.045–0.075	2.97±0.83	5.80±1.97		1.39±0.07	2.84±0.14	0.01±0.00	1.93	0.70±0.01	4.24±1.25	8.28±2.93	
	0.075–0.100	3.88±0.86	17.87±3.76						0.65±0.01	5.97±1.41	27.49±6.20	
	0.100–0.150	4.66±1.99	12.08±1.71						0.62±0.01	7.52±3.33	19.48±3.08	
B1	0.045–0.075	3.54±0.41	8.30±1.24		4.23±0.08	18.95±3.88	3.30±0.05	0.95	5.96±0.30	0.59±0.10	1.39±0.28	
	0.075–0.100	12.58±5.37	19.84±7.17						5.69±0.20	2.21±1.03	3.49±1.38	
	0.100–0.150	7.07±3.01	26.75±9.26						5.57±0.20	1.27±0.59	4.80±1.85	
	0.150–0.250	9.62±3.79	23.46±9.43						5.40±0.20	1.78±0.76	4.34±1.90	
	0.250–0.500	22.15±10.38	29.60±12.33						5.16±0.20	4.29±2.18	5.74±2.63	
	0.500–1.00	36.84±2.94	19.37±7.20						4.73±0.20	7.79±3.99	4.09±1.69	
B	0.045–0.075	11.44±2.52	8.86±1.93	12.24±2.22	4.01±0.10	23.29±0.80	Not determined	0.80	3.49±0.04	3.28±0.76	2.54±0.58	3.51±0.67
	0.100–0.150	8.53±14.59	10.15±2.86	13.33±3.40					3.11±0.04	2.74±4.72	3.26±0.96	4.28±1.16
	0.150–0.250	8.68±33.49	8.68±1.28	11.00±3.50					2.99±0.04	2.90±11.23	2.90±0.47	3.68±1.21
	0.250–0.500	11.61±2.39	7.84±1.23	8.49±2.78					2.89±0.04	4.02±0.90	2.41±0.47	2.94±1.00
	0.500–1.00	75.72±5.65	8.54±0.56	12.20±3.65					2.75±0.04	27.53±2.47	3.11±0.25	4.44±1.40
D1 (HF)	0.045–0.075	8.60±4.04	4.83±0.79		1.69±0.03	10.27±0.28	1.46±0.03	5.26	2.30±0.02	3.74±1.79	2.10±0.36	
E1 (HF)	0.020–0.045	6.32±1.63	13.46±2.80		1.62±0.03	10.70±0.67	1.09±0.02	22.10	1.63±0.03	3.88±1.08	8.26±1.89	
N	<0.045	2.34±0.27	13.74±5.80		0.04±0.00	12.54±0.84	Not determined	1.76	1.50±0.04	1.56±0.22	9.16±4.09	
	0.045–0.075	11.59±9.34	17.01±3.37						1.24±0.04	9.35±7.88	13.72±3.16	
	0.075–0.100	19.91±4.44	16.39±5.60						1.22±0.04	16.32±4.13	13.43±5.01	
	0.100–0.150	18.40±7.63	14.14±3.20						1.07±0.04	17.20±7.87	13.22±3.48	
	0.150–0.250	11.83±5.71	4.22±1.77						1.03±0.04	11.49±5.96	4.09±1.87	
	0.250–0.500	30.67±7.36	2.49±0.36						1.00±0.04	30.67±8.59	2.49±0.45	

3. Results

D_E values and ages in addition to their associated errors were calculated for all observable centres in the samples using the variations of the ESR intensities. The results are presented for all samples with the different grain sizes in Table 2. Fig. 5a–e shows D_E values vs. grain size for B1, B, GG, GOK from the NAF and N from the NF. GOK yielded results only for the sizes of 0.045–0.075, 0.075–0.100 and 0.100–0.150 mm.

3.1. Grain size plateau method

3.1.1. Samples from the NAF

D_E values of the Al centres in B1 and GOK are found to decrease with decreasing grain size (Fig. 5a and d) and in B and GG (Fig. 5b and c) the A1-D_E values have plateaux to the size of 0.25–0.50 and 0.075–0.1 mm, respectively; then they increase by increasing sizes. The E′ centre shows no consistent trend in D_E with grain size. The D_E values of this centre in GG yield a plateau

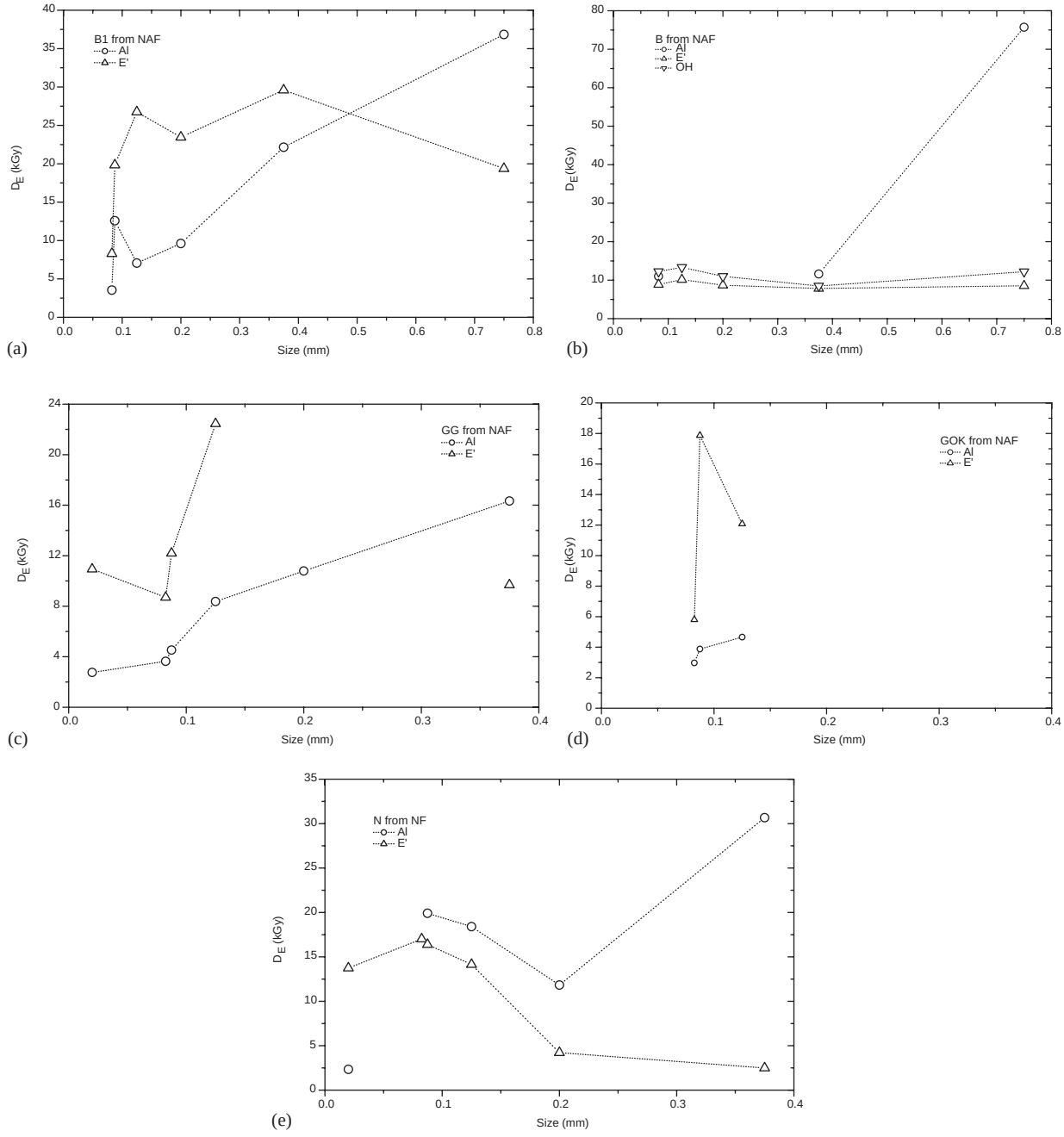

Fig. 5. Obtained D_E values grain size for Al, OH and E′ centres in the samples of (a) B1, (b) B, (c) GG, (d) GOK from the NAF and (e) N from the NF.

for the sizes of 0.045–0.075 to 0.075–0.100 mm, and then increase for 0.100–0.150 mm followed by a decrease for larger sizes, while those in GOK increase to 0.075–0.100 mm and then decrease for larger grains. The E′ values increase with increasing sizes to 0.100–0.150 mm and then reach a plateau for B1, while those of E′ and OH centres in B do not change by the sizes in a wide range.

B1 and GOK show neither well-defined plateaus nor congruent D_E values for the Al and E′ centres in the finest grain site though they have similar variations. The D_E values for Al and E′ centres in GG have plateaux in the finer grains though the plateaux do not come close to each other. The Al, E′ and OH centres in B show well-defined plateaux at a congruent value meaning that this sample may have been completely reset.

Fig. 6a–d shows the calculated ages vs. grain size for these centres. The trends of variation in D_E with grain size and the differences between various ESR signals are reproduced in the ages, although the ages do not show a strict relation to D_E.

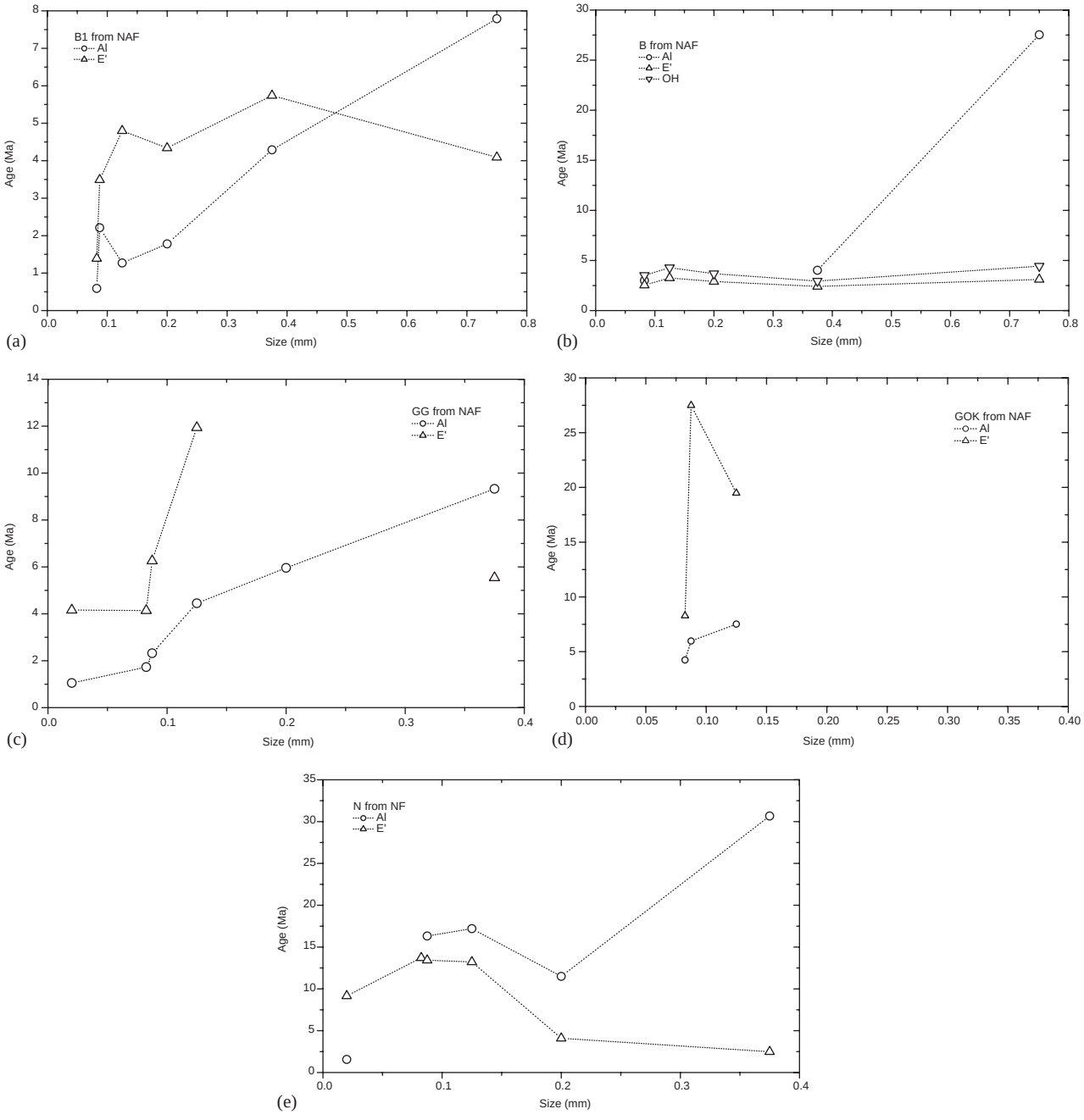

Fig. 6. Age values grain size for Al, OH and E′ centres in the samples of (a) B1, (b) B, (c) GG, (d) GOK from the NAF and (e) N from the NF.

3.1.2. Samples from the NF

D_E values of the Al centres in N decrease with decreasing grain size in Fig. 5e, while those of the E′ centres increase with increasing sizes to 0.100–0.150 mm and then decrease for larger grains. The trends of variation in the calculated ages for the Al and E′ centres with grain sizes are shown in Fig. 6e. The age of the Al decreases to 1.56 ± 0.22 Ma for the finest grain site though that of the E′ centre is close to 9.16 ± 4.09 Ma.

3.2. Fault gauge isochron method

D_E values of the same samples are investigated as a function of the external dose rates, which increase with decreasing grain sizes (Table 2). Fig. 7a–d shows the variations of D_E as a function of dose rate for each grain size assuming an α-efficiency of $k = 0.07$ and incorporating the corrections for α- and β-attenuation due to grain size. The E′ centre in sample N is the only data set that shows increasing dose values with increasing dose rates (=decreasing grain size). All other results are either inconclusive or shows a reverse trend.

4. Discussion

The results of the centres in the samples are mostly consistent with the grain size plateau model suggesting that finer grains are more thoroughly reset than larger ones during fault movements. The fault gouge isochron method seems to work only for the E′ centres in N for the grain sizes of 0.25–0.50 to 0.10–0.15 mm. The D_E values and ESR ages of the Al centre in all samples are consistent with the results of experimental studies of the resetting of ESR signals, which showed that finer grains are more reset than larger ones during shearing (Buhay et al., 1988; Lee and Schwarcz, 1994). This was also supported using Al and Ti centres in different grain sizes of quartz extracted from volcanic sediments in Kapadokya–Turkey (Ulusoy, 1995; Ulusoy et al., 1996). During these events, two mechanisms, deformation of the quartz crystals and local heating at grain-grain contacts may cause the release of trapped charges.

4.1. Samples from the NAF

Only the D_E values of the Al centre in B from the depth of 245 m at the Düzce Fault give a plateau over a

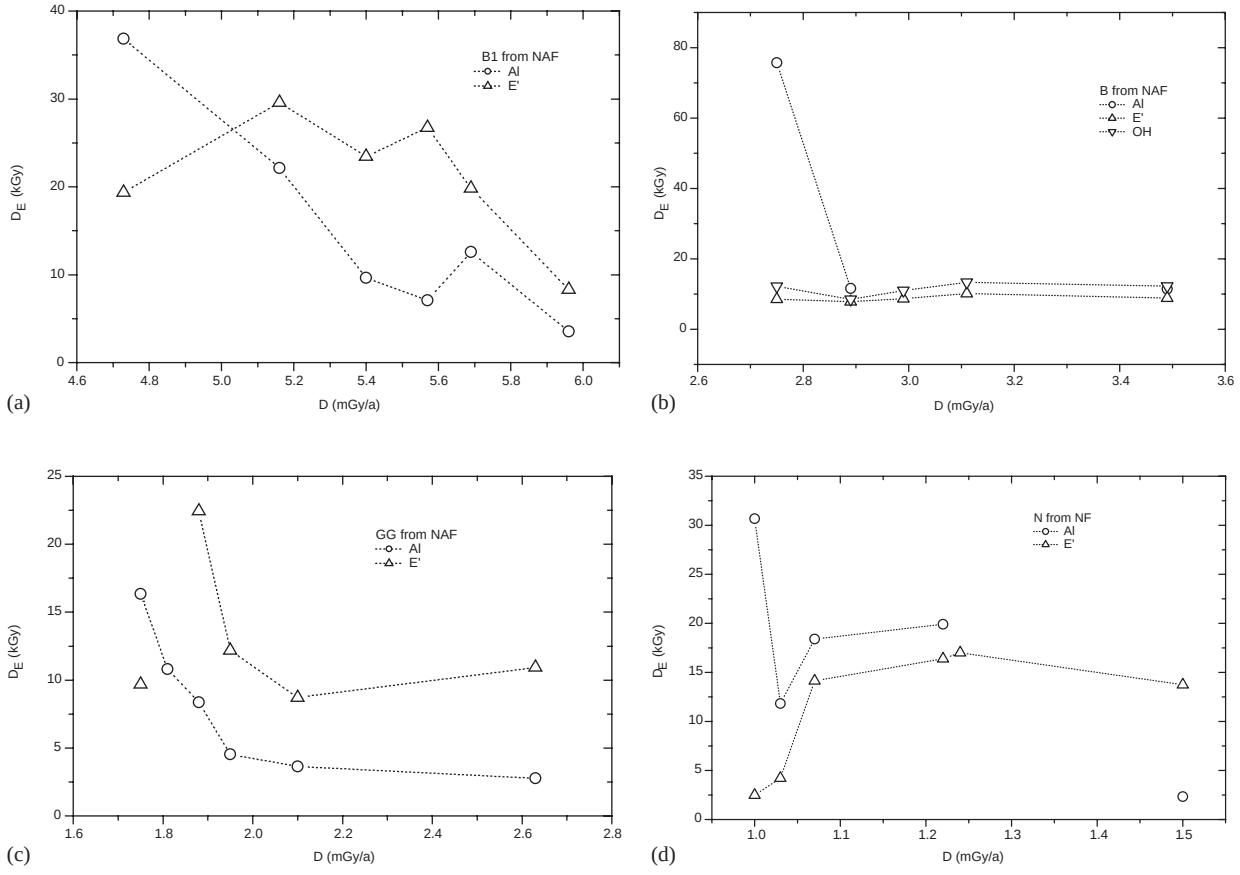

Fig. 7. D_E of grain size as a function of the calculated external dose rate taking into account the correction factors of α- and β-rays. The variations did not support the ESR isochron dating hypothesis except for E′ centres in N. (a) B1, (b) B, (c) GG from the NAF and (d) N from the NF.

wide particle range, 0.25–0.50 mm before increasing, while those of E′ and OH centres are uniform for all sizes (Fig. 5b). The lowest D_E values for Al, E′ and OH are found between 8.86 ± 1.93 and 12.24 ± 2.22 kGy. These correspond to the ages between 2.54 ± 0.58 and 3.51 ± 0.67 Ma. The plateaux indicate complete resetting and the obtained age may be accepted as the time of initial fault movement.

Al and E′ centres in B1 from the depth of 190 m show the expected decrease in D_E with decreasing grain size, although they do not display any plateaux. For this sample, the smallest grain sizes give convergent dose values to 3.54 ± 0.41 and 8.30 ± 1.24 kGy, which corresponds to the ages of 0.59 ± 0.10 and 1.39 ± 0.28 Ma for Al and E′ centres, respectively.

The ages of D1(HF) and E1(HF) samples with the finest grains from the depths of 170 and 90 m at a different place of the same fault was calculated as 3.74 ± 1.79 and 3.88 ± 1.08 Ma for Al, and 2.10 ± 0.36 and 8.26 ± 1.89 Ma for E′ centres, respectively (see Table 2).

B1 is the youngest sample of the Düzce Formation with ages of 0.59 ± 0.10 and 1.39 ± 0.28 Ma for Al and E′ centres. These ages give perhaps the time of the last movement of one of the strands at this fault. The oldest ESR ages for the Al in the largest grains in B and B1 at the Düzce Fault are calculated as 27.53 ± 2.47 and 7.79 ± 3.99 Ma, while those for the E′ centres are obtained 3.11 ± 0.25 and 4.09 ± 1.69 Ma, respectively. Additionally, the ages of the OH centres are calculated as 3.51 ± 0.67 and 4.44 ± 1.40 Ma for the finest and largest grains. The ages of the A1 centre in the large grains indicate the older age of the Düzce formation, which was formed during the Upper Cretaceous (Demirtaş, 2000).

Al and E′ centres in the finest grains of GG from the surface at the Mudurnu Fault display two plateaux at different D_E values, 2.76 ± 0.80 and 10.94 ± 2.76 kGy, respectively. The values show that Al centres change most sensitively with grain size and might be reset more easily than E′ centres. The ages, 1.05 ± 0.31 and 4.16 ± 1.08 Ma for Al and E′ centres are about the same as the ages of 1.03 ± 0.19 and 4.46 ± 1.48 Ma for the other sample, GK(HF), from the same place with the different properties. The ages of the Al centres in GG and GK(HF) may be a more reliable age estimate of the fault movement. The ages of larger grains of GG are apparent ages due to partial resetting of ESR signals during faulting.

The last sample, GOK from the Gökören at the Mudurnu Fault, displays neither plateaux nor congruent D_E values for Al and E′ centres. To judge this result obtained for only three different grain size groups, the experiments should be expanded to several size groups. The ages of GOK for the finest grains are found to be 4.24 ± 1.25 and 8.28 ± 2.93 Ma for Al and E′ centres respectively. They are somewhat older than the age of the Arkotdağ Formation or Arkotdağ Complex (1.97–2.36 Ma) in which the Mudurnu Fault must have been developed since this time.

4.2. Samples from the NF

The D_E values and ages for the Al centres tend to increase by increasing sizes while those for the E′ centres decrease by decreasing sizes. Thus, it can be said that the behaviours of the D_E values and ages of Al are consistent with "the grain size method", while those of E′ centre follow "the fault gouge isochron method". The variations in ESR ages for the E′ centres are different to those of the Al and E′ centres in the other samples. Toyoda and Schwarcz (1997a, b) have found that γ-ray irradiation of granitic quartz produces a distinct ESR signal which overlaps the E′ centre signal. It is known as the counterfeit E′ signal and can be removed by heat treatment at 170°C for 15 min. The contribution of the counterfeit E′ signal to the total apparent E′ centre signal intensity is significiant and appears to account for most of the growth of the combined signal with irradiation. The occurrence of the counterfeit signal may lead to significant erroneous dose estimation even if the dose range applied is small. In this research, we did not heat our samples and examined whether the real E′ signal had been overlapped, and consider the contribution of the counterfeit E′ signal to the signal intensity. The differences in the D_E values for E′ and Al centres may be caused by the counterfeit E′ signal. The counterfeit signal may also explain why "the fault gouge isochron method" apparently worked for only one sample in granitic quartz grains in the fault gouge at the outcrop of the Rokko Fault in Japan (Ikeya et al., 1995). These researchers did not heat their samples and apply this method to any other centres in their work.

The age of the Al centres for the finest grains of N, 1.56 ± 0.22 Ma is close to the one of the E′ centres for the largest grains, 2.49 ± 0.45 Ma. Geological research has shown that Awaji Island started to uplift approximately 1.2 Ma ago mainly by movements of the NF in addition to the Asano, Kusumoto and the Higashiura Faults. Therefore, the age of the centre of the finest grains is consistent with the initial movements of the NF.

None of the samples show any centres, which were completely reset during the recent fault movements. In fact, the ESR ages of sample N, which was collected from the surface outcrops of the NF gouge at Hirabayashi after the Kobe Earthquake in 1995, were expected to be younger than 1.56 Ma since the Al and E′ centres might have been annealed during this earthquake. However, Fukuchi (1996a, b) and Fukuchi and Imai (1998) showed that the ESR signals in the samples from the same site had hardly been affected at all by

recent faulting. On the other hand, Fukuchi (1992) pointed out that complete resetting of ESR signals by frictional heating occurs only at deep sites. Other ESR experiments were carried out on the fault gouge in the DPRI (Disaster Prevention Research Centre, Kyoto University) recovered from a 500 m drill core (Fukuchi and Imai, 2001). These experiments showed that the hyperfine structure of an Al centre in quartz had been reduced to 31–36% of the initial intensity by heating, whereas an E′ centre in quartz had only been reduced to 70%. These results mean that ESR ages of fault gouge collected from a depth of less than 388 m does not give the age of the latest fault movement.

In the other research, all ESR signals in quartz disappear after 1 h isochronal annealing in the range of 300–400°C (Shimokawa and Imai, 1987; Yokoyama et al., 1985). Many workers have reported that very high temperatures are being reached on experimental faulting tests. However, theoretical calculations performed for real faulting situations yielded temperatures between 150–200°C, well below the temperatures needed for total resetting of the ESR signals (Buhay et al., 1988). Matsumoto et al. (2001) conducted studies to assess the heating history at faulting by analyzing the spatial distribution of defect centres in the samples from the fault plane surface of the NF at the depth of 389.4 m. They found that the ESR signal was not zero even on the fault plane at this depth. However, the profiles of defect concentration clearly showed a potential annealing effect near the fault plane.

It is clear from the results of our ESR experiments that the degree of resetting is dependent on grain size and that the grain size plateau method, which contradicts the fault gouge isochron method, works well. Smaller quartz particles gave smaller equivalent doses, which indicates that these had been annealed more during faulting. Finally, we would like to emphasize the importance of the grain size method in relation to complete zeroing, although the conditions of complete annealing could not be found for the samples even from the fault plane surface. New suggestions for ESR fault dating, without assuming complete annealing during faulting, should be examined in the future experiments.

Acknowledgements

I gratefully thank Geo. Eng. Y. Yılmaz who has been working for Astaldi Company during the construction of the Bolu Tunnel and Dr. Ü. Dikmen (the Ministry of Public Works and Settlement, General Directorate of Disaster Affairs, Earthquake Research Department, Ankara) for helping me to collect fault gouge samples and to prepare the maps. I would also like to extend my thanks to Prof. M. Ikeya for giving me the opportunity to conduct this study at his Quantum Geophysics Laboratory (Department of Earth and Space Science, Graduate School of Science at Osaka University) and also all the members of this laboratory; Dr. H. Matsumoto, Dr. A. Tani, Mr. D. Yoshida, Mr. H. Sato for helpful discussions and their technical assistance and Prof. N. Whitehead for his help in improving the original manuscript. This research was supported by TUBİTAK from Turkey.

References

Arai, R., Takemura, K., 2001. Fission-track ages of the volcanic ash layers in the Osaka Group, northwest part of Awaji Island, Japan. Journal of the Geological Society of Japan, in press (in Japanese).

Aydan, Ö., Ulusay, R., Kumsar, H., Tuncay, E., 2000. Site investigation and engineering evaluation of the Düzce-Bolu Earthquake of November 12, 1999. Turkish Earthquake Foundation, Earthquake Report, TDV/DR 09-51, 220pp.

Bar, M., Kolodny, Y., Bentor, UK, 1974. Dating of faults by fission track dating of epidotes. An attempt. Earth and Planetary Science Letters 22, 157–166.

Barka, A.A., 1981. Seismotectonic aspects of the North Anatolian Fault zone. Ph.D. Thesis, University of Bristol, England, 335pp.

Bell, W.T., 1980. Alpha dose attenuation in quartz grains for thermoluminescence dating. Ancient TL 12, 4–8.

Buhay, W.M., Schwarcz, H.P., Grun, R., 1988. ESR dating of fault gouge: the effect of grain size. Quaternary Science Reviews 7, 515–522.

Demirtaş, R., 2000. Paleoseismicity and neotectonics of the Abant-Gerede Region of the North Anatolian Fault zone. Ph.D. Thesis, Ankara University, Turkey, 191pp. (unpublished).

Eyal, Y., Kaufman, A., Matthews, M.B., 1992. Use of 230Th/U ages of striated carnotites for dating fault displacements. Geology 20, 829–832.

Falgueres, C., Yokoyama, Y., Miallier, D., 1991. Stability of some centres in quartz. Nuclear Tracks and Radiation Measurements 18 (1/2), 155–161.

Fukuchi, T., 1988. Applicability of ESR dating using multiple centres to fault movement—the case of the Itoigawa–Shizuoka Tectonic Line, a major fault in Japan. Quaternary Science Reviews 7, 509–514.

Fukuchi, T., 1989a. Increase of radiation sensitivity of ESR centres by faulting and criteria of fault dates. Earth and Planetary Science Letters 94, 109–122.

Fukuchi, T., 1989b. Theoretical study on frictional heat by faulting using ESR. Applied Radiation and Isotopes 40 (10– 12), 1181–1193.

Fukuchi, T., 1992. ESR studies for absolute dating of fault movements. Journal of the Geological Society of London 149, 265–272.

Fukuchi, T., 1996a. Quartet ESR signals detected from natural clay minerals and their applicability to radiation dosimetry and dating. Japanese Journal of Applied Physics 35, 1977–1982.

Fukuchi, T., 1996b. Direct ESR dating of fault gouge using clay minerals and the assessment of fault activity. Engineering Geology 43, 201–211.

Fukuchi, T., Imai, N., 1998. ESR isochron dating of the Nojima Fault Gauge, southwest Japan, using ICP-MS: an approach to fluid flow events in the fault zone. In: Parnell, J. (Ed.), Dating and Duration of Fluid Flow and Fluid–rock Interaction, Vol. 144. London Special Publications, Geological Society, pp. 261–277.

Fukuchi, T., Imai, N., 2001. ESR and ICP analyses of the DPRI 500 m drill core samples penetrating through the Nojima Fault, Japan. Island Arc 10, 465–478.

Grün, R., 1989. Electron spin resonance dating. Quaternary International 1, 65–109.

Ikeda, S., Ikeya, M., 1992. ESR signals in natural and synthetic gypsum: an application of ESR to the age estimation of gypsum precipitates from San Andreas Fault. Japan Journal of Applied Physics 31, L136–L138.

Ikeya, M., 1988. Dating and radiation dosimetry with ESR. Magnetic Resonance Review 13, 91–134.

Ikeya, M., 1993. New Applications of Electron Spin Resonance—Dating, Dosimetry and Microscopy. World Scientific, Singapore.

Ikeya, M., Miki, T., Tanaka, K., 1982. Dating of a fault by ESR on intrafault materials. Science 215, 1392–1393.

Ikeya, M., Tani, A., Yamanaka, C., 1995. Electron spin resonance isochrone dating of fracture age: grain-size dependence of dose rates for fault gouge. Japan Journal of Applied Physics 34, L334–L337.

Imai, N., Shimokawa, K., Hirota, M., 1985. ESR dating of volcanic ash. Nature 314, 81–83.

Ketin, I., 1968. Relation between general tectonic features and the main earthquake region of Turkey. Bulletin of the Mineral Research and Exploration Institute 71, 63–67.

Ketin, I., 1969. On the North Anatolian Fault. Bulletin of the Mineral Research and Exploration Institute 72, 1–26.

Kralik, M., Clauer, N., Holnsteiner, R., Huemer, H., Kappel, F., 1992. Recurrent fault activity in the Grimsel Test Site: revealed by Rb–Sr, K–Ar and tritium isotope techniques. Journal of Geological Society of London 149, 293–301.

Lee, H.K., Schwarcz, H.P., 1994. Criteria for complete zeroing of ESR signals during faulting of the San Gabriel fault zone, southern California. Tectonophysics 235, 317–337.

Matsumoto, H., Yamanaka, C., Ikeya, M., 2001. ESR analysis of the Nojima fault gouge, Japan, from the DPRI 500 m borehole. Island Arc 10, 479–485.

Mejdahl, V., 1979. Thermoluminescence dating: beta-dose attenuation in quartz grains. Archaeometry 21, 61–72.

Miki, T., Ikeya, M., 1982. Physical basis of a fault dating with ESR. Naturwissenschaften 69, 390–391.

Murata, A., Takemura, K., Miyata, T., Lin, A., 2001. Quaternary vertical offset and avarage slip rate of the Nojima Fault on Awaji Island, Japan. Island Arc 10, 360–367.

Ogoh, K., Ikeda, S., Ikeya, M., 1993. Adv. ESR Applications 9, 22.

Şaroğlu, F., Emre, Ö., Kuşcu, İ., 1992. Active fault map of Turkey. MTA-General Directorate of Mineral Research and Exploration, Ankara-Turkey (scale: 1/1000000).

Schwarcz, H.P., Buhay, W.M., Grun, R., 1987. ESR dating of fault gouge. In: Crone, A.J., Olmdahl, E. (Eds.), Directions in Paleoseismology. US Geological Survey, Open File Report, Vol. 87–673, pp. 50–64.

Shimokawa, K., Imai, N., 1987. Simultaneous determination of alteration and eruption ages of volcanic rocks by electron spin resonance. Geochimica et Cosmochimica Acta 51, 115–119.

Shimokawa, K., Imai, N., Hirota, M., 1984. Dating of a volcanic rock by electron spin resonance. Isotope Geoscience 2, 365–373.

Tadokoro, K., Nishigami, K., Ando, M., Hirata, N., Iidaka, T., Hashida, Y., Shimazaki, K., Ohmi, S., Kano, Y., Koizumi, M., Matsuo, S., Wada, H., 2001. Seismicity changes related to a water injection experiment in the Nojima Fault Zone. Island Arc 10 (3/4), 235–243.

Tanaka, H., Hinoki, S., Kosaka, K., Lin, A., Takemura, K., Murata, A., Miyata, T., 2001. Deformation mechanism and fluid behaviour in a shallow, brittol fault zone during coseismic and interseismic periods: results from drill core penetrating the Nojima Fault, Japan. Island Arc 10 (3/4), 381–391.

Toksöz, M.N., Shakal, A.F., Michael, A.J., 1979. Space–time migration of earthquakes along the north Anatolian Fault zone and seismic gaps. Pure and Applied Geophysics 117, 1258–1270.

Toyoda, S., Ikeya, M., 1991. Thermal stabilities of paramagnetic defect and impurity centres in quartz: basis for ESR dating of thermal history. Geochemical Journal 25, 437–445.

Toyoda, S., Schwarcz, H.P., 1997a. Counterfeit E1' signal in quartz. Radiation Measurements 27 (1), 59–66.

Toyoda, S., Schwarcz, H.P., 1997b. The hazard of the counterfeit E1′ in quartz to the ESR dating of fault movements. Quaternary Science Reviews (Quaternary Geochronology) 16, 483–486.

Ulusoy, Ü., 1995. ESR studies and dating of quartz minerals. Ph.D. Thesis, Hacettepe University, Turkey, 99pp. (in Turkish).

Ulusoy, Ü., 2000. ESR dating of a quartz single crystal from the Menderes Massif in Turkey. Applied Radiation and Isotopes 52, 1363–1370.

Ulusoy, Ü., Kaptan, Y., Apaydın, F., 1996. ESR dating and thermal behaviour of the Al and Ti centres in quartz. Turkish Journal of Physics 20, 1141–1148.

Yokoyama, Y., Falgueres, C., Quaegebeur, J.P., 1985. ESR dating of quartz from Quaternary sediments first attempt. Nuclear Tracks 10, 921–928.